TECHNICAL ARTICLE

Numerical Validation of the Incremental Launching Method of a Steel Bridge Through a Small-Scale Experimental Study

R. Chacón[1], N. Uribe[1], and S. Oller[2]

1 Construction Engineering Department, Universitat Politècnica de Catalunya. Barcelona Tech, Barcelona, Spain
2 International Centre for Numerical Methods in Engineering (CIMNE), Universitat Politècnica de Catalunya. Barcelona Tech, Barcelona, Spain

Keywords
Incremental Launching Method, Steel Bridges, Bridge Monitoring

Correspondence
R. Chacón,
Construction Engineering Department
Universitat Politècnica de Catalunya.
Barcelona Tech
Barcelona, Spain
Email: rolando.chacon@upc.edu

Received: July 3, 2013;
accepted: November 7, 2013

doi:10.1111/ext.12069

Abstract

This article presents an experimental and a numerical study of an incremental launching process of a steel bridge. The former is deployed in a scale-reduced laboratory, whereas the latter is performed using the finite element method. The numerical simulation is based upon realistic transient boundary conditions and accurately reproduces the elastic response of the steel bridge during launching. This numerical approach is validated experimentally with the scale-reduced test performed at the laboratory. The properly validated numerical model is subsequently systematically employed as a simulation tool of the process. The proposed simulation protocol might be useful for design and monitoring purposes of steel bridges to be launched. Results concerning strains, stresses, and displacements might be inferred from the model and thus compared to field measurements obtained in situ. The conditions presented at the end of the article are potentially useful for researchers and practice engineers alike.

Introduction

The incremental launching method (ILM) has gained increasing popularity in last decades as a construction method of short- to large-multispanned steel and/or concrete bridges.[1] ILM consists of assembling the superstructure on one side of the obstacle to be crossed and then pushed longitudinally (or ''launched'') into its final position. Generally, steel bridges are completely assembled prior to launching operations. In concrete bridges, however, the launching is typically performed in a series of increments so that additional sections can be added to the rear of the superstructure unit prior to subsequent launches. The ILM may offer advantages over conventional construction techniques when the construction takes place in environmentally protected areas, or areas at which minimal disturbances to surroundings are needed, thus providing a more concentrated work area for the superstructure assembly. Safety concerns might also be reduced if ILM is employed.[1−3] During the launching operation, the bridge superstructure is supported by a series of rollers or sliding bearings. The thrust required to launch the bridge forward can be provided by a variety of jacking systems, including hydraulic pistons or hollow-core strand jacks.[1] Figure 1 shows a lateral schematic view of an incrementally launched steel girder. It is worth pointing out the continuous change of the static conditions. In Fig. 1, the varying bending moment diagrams are qualitatively included for illustration.

The ILM has reportedly been used for the first time in Venezuela during 1960s for a bridge over the Caroni River.[3] Ever since that hundreds of steel and/or concrete bridges have been built worldwide using the ILM. A close inspection of the vast database given in Ref. 1 gives a worth mentioning twofold observation: Europe has a vaster tradition of systematic usage of ILM than the USA and the vast majority of launched bridges are made of post-tensioned concrete.

Admittedly, according to Ref. 1, there has historically been a knowledge gap between designers, contractors, and bridge owners when it comes to the systematic usage of ILM. ILM requires a considerable amount of analysis and design expertise and specialized construction equipment. A detailed structural

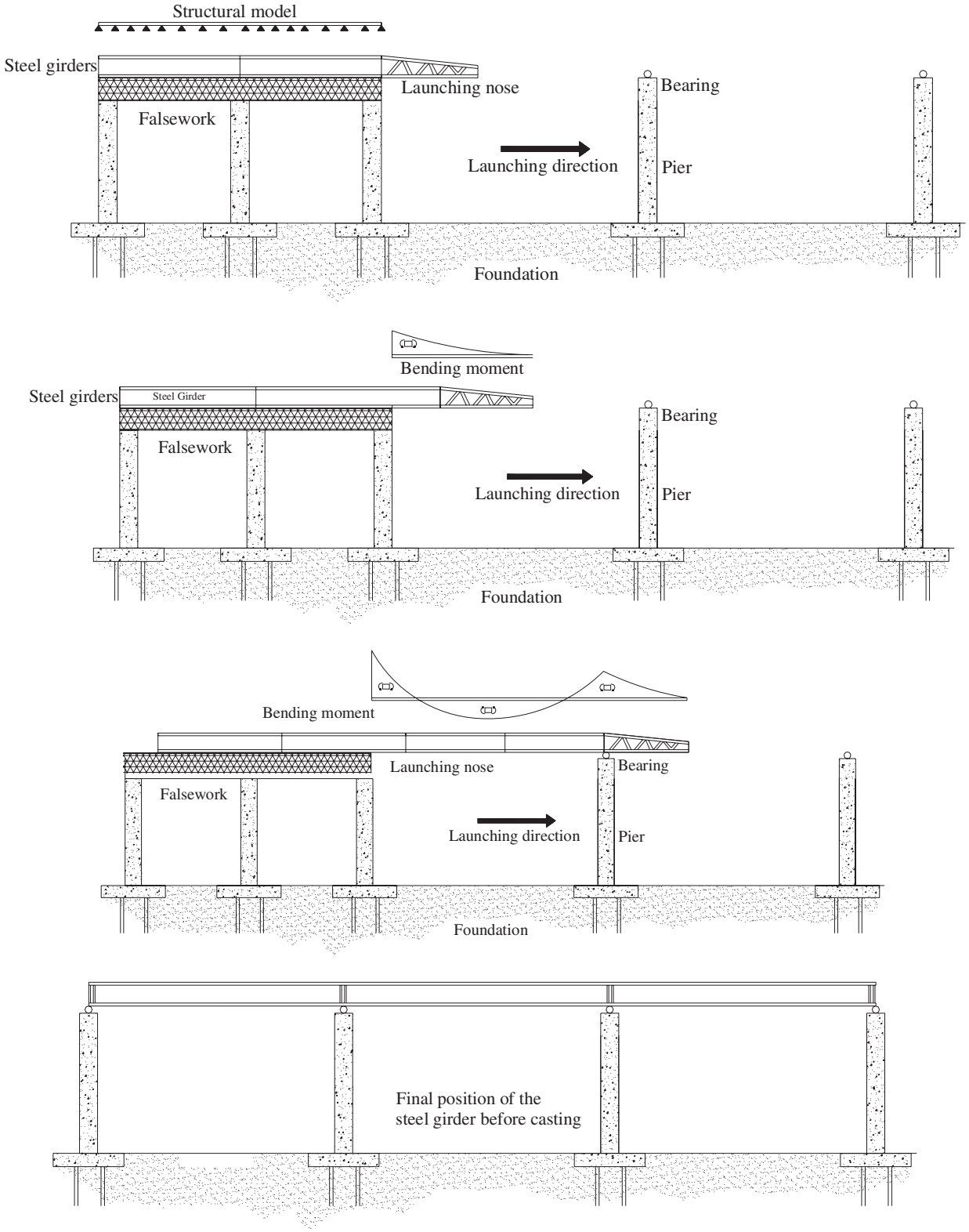

Figure 1 Incremental launching method of a steel bridge.

analysis of all construction phases is compulsory. It is necessary to take into account the continuous change of the structural scheme due to the transient conditions of the supports. Internal as well as external forces acting on the rollers might considerably change throughout the process. The stress state at the final phase of the bridge girders might differ considerably (in magnitude and sign) from the stress states that have been carried out during launching. Furthermore, it is a matter of fact that the launching of bridges made of concrete requires a different set of solutions than those required for purely metallic bridges. For the former, the design of the post-tensioning system must consider not only dead load stresses but also the considerable stress reversals that occur during launching. For the latter, there are a number of issues related to large concentrated forces applied to the girder (namely, patch loading) as well as to the torsional stiffness of an open section, such as an I-girder, that must be carefully addressed by the designer in order to avoid an undesired instability-related collapse.

This article presents numerical- and scale-reduced experimental reproductions of a steel bridge whose construction process is the ILM. The numerical reproduction is performed using a FE-based commercial software that is properly validated with a scale-reduced model deployed at the Laboratory of the Chair of Strength of Materials-Technical University of Catalonia (UPC). The numerical model is based upon a contact formulation and allows to reproduce the continuous change of the boundary conditions of the launched girders. The results provided by the numerical model include stresses, strains, displacements, and support reactions that might be compared in situ with field measurements during the whole process. These comparisons might be of the utmost importance for control and monitoring engineers. Consequently, the results presented at the end of the paper are aimed at showing relevant information for designers, contractors, and bridge owners alike.

State of the Art

The ILM has been depicted quite thoroughly during the last decades in several books and papers available in the literature that address this topic with a broad perspective.[1−6] More specific papers concerning particular topics of the method have continuously been published. Rosignoli has focused his research to the design of the bridges, the launching noses and the rolling devices,[7−11] whereas Granath has pointed out the structural response of particular elements of the steel bridges that are exposed to concentrated loads of considerable magnitude.[12−14] On the other hand, several publications related to bridges constructed using the ILM are available.[1,15−17]

Publications related to the numerical simulation of incrementally launched steel bridges are, however, rather scarce. Marzouk et al.[18] performed several applications of computer simulations of incrementally launched bridges. Their main purpose was to improve the design of the bridge to be launched by developing optimization algorithms. Ronggiao and Shao[19] developed a new beam finite element suitable to reproduce the continuous changes in the support conditions when a superstructure is constructed using the ILM.

Moreover, it has been of the utmost importance to monitor steel bridges while being launched. During the launching phase, the process is usually monitored via reaction at supports/rollers or via displacement using topography equipment.[2] These controls are discretely measured in regions that are anticipated to be somewhat critical. Recently, Chacón et al.[20] performed a research work aimed at monitoring the strain levels of the steel girders with wireless sensors. The results have been useful at research levels showing that wireless technology might be considerably useful during such construction process. Other researchers have already implemented monitoring deployments over incrementally launched steel bridges with various levels of accuracy and/or amount of collected data.[21−23] Publications related to computer-aid design and visualization of launched bridges are also available.[24]

Scale-Reduced Experimental Simulation of the ILM

General

An experimental reproduction of an incremental launching procedure of a steel bridge was deployed at the Laboratory of the Chair of Strength of Materials-Technical University of Catalonia (UPC). The objective was to reproduce a launching procedure of a medium-multispanned bridge assembled with steel I-girders. This prototype is a standard design routinely employed in road bridges.[25] The chosen geometry for the reproduction is a laterally restrained, steel multi-I-girder whose final configuration is a continuous and symmetric two-spanned multi I-girder beam with a total length of 150 m and a single central pier (Fig. 2). The generic cross-section dimensions of the analyzed girder are also included. For the sake of simplicity, only one girder (bolded in Fig. 2) is considered in the analysis. The other girders are displayed in dashed lines only for illustration purposes.

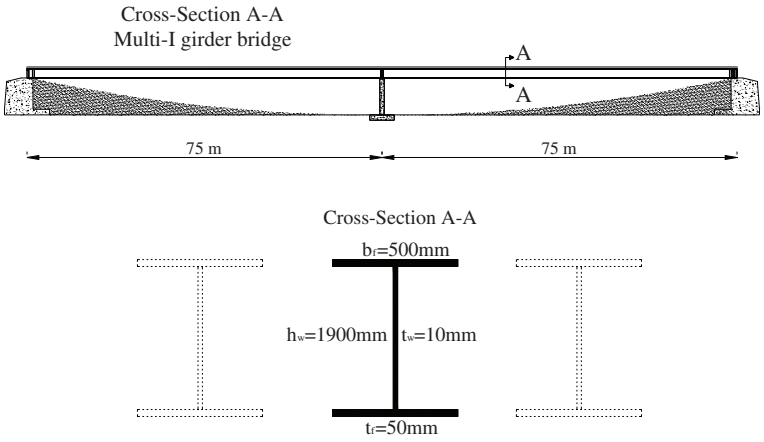

Figure 2 Prototype longitudinal and transversal view.

The depicted prototype was scale-reduced for a proper adaptation to the laboratory facilities. The reduced model was inferred from a thorough comparison between the prototype geometry, the laboratory facilities, and by applying the PI-Buckingham theorem.[26,27] The theorem roughly states that a physically meaningful equation (in this case, structurally meaningful) involving a certain number n of parameters is equivalent to an equation involving a set of $p = n - k$ dimensionless parameters constructed from the original variable (being k the number of independent fundamental physical quantities).

Table 1 shows the considered n structural parameters (including numerical values), whereas Table 2 shows the p chosen dimensionless groups. Thus, the prototype was structurally scale-reduced to the experimental model.

A close inspection of Tables 1 and 2 leads to pinpoint a threefold observation:

- Dimensionless groups 7 and 9 define the scale-reduced model geometry, that is to say, the ratio between vertical displacement and the span length.

Table 1 Structural parameters

Symbol	Description	SI units	Prototype	Scale-reduced model
E	Elasticity modulus	N/mm^2	210,000	210,000
ν	Poisson's ratio	–	0.3	0.3
L	Span length	m	75	1
Q	Self-weight	kN/m	5.42	1.88×10^{-2}
M	Bending moment	kN m	15.23	9.42×10^{-3}
σ	Stress	N/mm^2	286	58.9
ϵ	Strain	–	1.43×10^{-3}	2.94×10^{-4}
δ	Vertical displacement	mm	2010	37
φ	Rotations at supports	rad	3.58×10^{-2}	4.91×10^{-2}
W	Section modulus	mm^3	53,257.5	160
F	Forces (Reactions)	kN	406.24	1.88×10^{-2}

Table 2 Dimensionless groups and similarity ratios

Dimensionless group	Similarity	Structural parameters	Dimensionless ratios	Scale factor
1	$\pi_1 - \pi'_1$	$\frac{F}{E \cdot l^2} = \frac{F'}{E' \cdot l'^2}$	$\lambda_f = \lambda_l{}^2$	$\left(\frac{1}{75}\right)^2$
2	$\pi_2 - \pi'_2$	$\nu = \nu'$	$\lambda_\nu = 1$	1
3	$\pi_3 - \pi'_3$	$\frac{q}{E \cdot L} = \frac{q'}{E' \cdot l'}$	$\lambda_l = \lambda_q$	$\left(\frac{1}{75}\right)$
4	$\pi_4 - \pi'_4$	$\frac{M}{p \cdot l} = \frac{M'}{p' \cdot l'}$	$\lambda_M = \lambda_l$	$\left(\frac{1}{75}\right)$
5	$\pi_5 - \pi'_5$	$\sigma = \sigma'$	$\lambda_\sigma = 1$	1
6	$\pi_6 - \pi'_6$	$\epsilon = \epsilon'$	$\lambda_\epsilon = 1$	1
7	$\pi_7 - \pi'_7$	$\frac{\delta}{l} = \frac{\delta}{l'}$	$\lambda_\delta = \lambda_l$	$\frac{1}{75}$
8	$\pi_8 - \pi'_8$	$\phi = \phi'$	$\lambda_\phi = 1$	1
9	$\pi_9 - \pi'_9$	$\frac{l^3}{w} = \frac{l'^3}{w'}$	$\lambda_w = \lambda_1{}^3$	$\left(\frac{1}{75}\right)^3$

- The self-weight is not considered in the structural variables as a mass force. The prototype and the scale-reduced model are made of the same material (steel). Therefore, both have identical values of density, Young's modulus, and Poisson's ratio.
- Strains, stresses, and Poisson's ratio (groups 2, 5, and 6) remained unaltered in the reduced model. These magnitudes do not play any role when calculating the scaled model geometry. However, from a simplified static analysis of the phenomenon, it was inferred and verified that the stresses obtained at any point on the steel plate should not exceed the yield point threshold.

In its final stage, the steel plate was a symmetric two-spanned continuous beam with a total length of 2000 mm and a rectangular 60×4 mm cross-section. This section is chosen for the sake of accomplishing the scale of the inertia (an I-beam would provide a major-axis inertia that would require a longer span). The steel plate was designed with a launching nose with the same cross-section and material. This plate was launched from one support another by means of

a roller system designed at the laboratory facilities. The length scale (pointed out in Table 2) was not precisely obtained since the cross-section had to be adapted the available commercial steel profiles.

Figure 3 depicts the rolling system, the rigid supports that provided the central pier, the dimensions of the launching nose as well as the end support. Figure 4 shows details A and B (displayed in Fig. 3) of the scale-reduced launching procedure. It is worth pointing out the following features:

- The rolling system was frictionless.
- Lateral restraints were added to the system for the sake of avoiding lateral displacements.
- The launching nose allowed the plate to reposition once the central and/or the end supports were approached by the launched steel plate.
- The launching was carried out as a series of increments with halts every 100 mm in order to minimize the potential effect of vibrations (especially in advanced cantilever phases prior to contact with the roller bearings).
- The test was repeated a statistically significant number of times (n = 30) and the results showed statistical consistency.

Measurements

Two types of measurements were collected during the launching procedure: strains and displacements at key points of the systems previously anticipated from theoretical calculations. For the former, two strain gages were bonded (longitudinally and transversely) at the point where the maximum longitudinal stress was expected (precisely at the center of the steel plate, see Fig. 4). The uni-axial gages (HBM K-RY81-6) were bonded only on the upper fiber of the steel plate to avoid any contact between roller and strain gage. For the latter, the vertical displacements of key points of the steel plate were collected by means of a photogrammetric procedure using a HD camera. The pictures were digitalized and scaled precisely. Accurate measurements were performed on the digital files. These results were further used to validate a numerical model. The strain results were collected with a Spider 8 data acquisition system. The signal was processed using the software CATMAN EASY 6.10.[28]

Experimental results

Strain

Figure 5 shows the results concerning the strain evolution on the top fiber of the steel plate during incremental procedure. The procedure as well as the plot are divided into five stages for readability:

- Zone A: The steel plate is supported by the rollers system, the measurement equipment was initialized, and the launching system was set up.
- Zone B: The launching procedure starts and the plate behaves like a cantilever with the upper fiber subjected to tensile stresses (positive in the plot). The maximum level of strain collected at this stage was 264 μm/m before the launching nose reached the central supports. Assuming that the Hooke's law governs the relationship between stresses and strain of the steel plate, the maximum stress recorded at this stage was approximately 54 N/mm^2.
- Zone C: The launching nose approaches the central support. The structural scheme suddenly changes and sign reversals of the internal forces are observed. During this stage the plate undergoes a

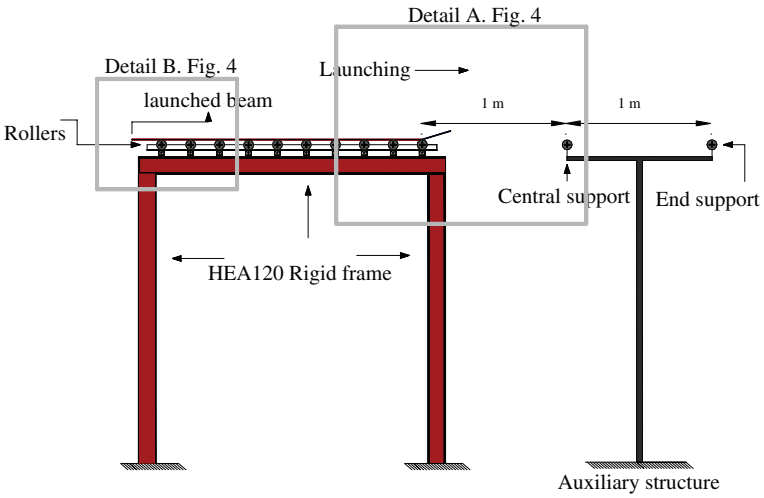

Figure 3 Laboratory test setup.

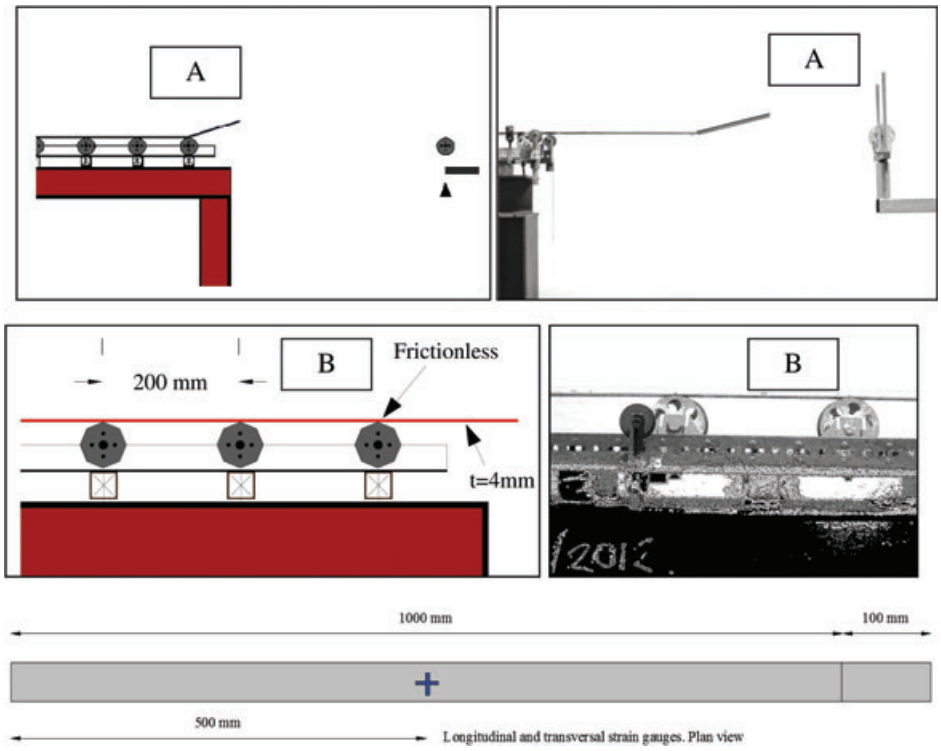

Figure 4 Details of the scale-reduced model.

sign reversal that ranges from the maximum tensile strain to the maximum compression strain at the top fiber (negative in the plot).

- Zone D: The launching procedure is continuously updated by the transient support conditions and the length of the cantilever which is formed at the second span. The longitudinal strain reaches a value of 264 μm/m (approximately 58 MPa of tensile on the top fiber) as it approaches the end support.
- Zone E: The launching nose reaches its final configuration. The steel plate forms a continuous two-spanned beam. It is worth mentioning that at this stage the registered strain level is considerably lower than the strain level recorded during launching. This fact shows the importance of a prior detailed structural analysis that depicts the launching procedure.

It is worth pointing out that as the stepwise nature of the experimentally collected data comes as a result of the elapsed time between successive increments of the experimental incremental launching procedure.

Vertical displacements

Figure 6 shows the schematic procedure that has been used for tracking the vertical displacement of the monitored point. The procedure consisted of placing a fixed HD camera that was shot regularly by means of a time-lapse application. The series of pictures were exported and treated with a CAD tool that allowed to measure the location of the monitored point with a high level of accuracy. Figure 7 shows the tracked vertical displacement at every step of 100 mm. In addition, the theoretical results of the vertical displacement of a similar system (the inclination of the launching nose of such system was disregarded for simplicity) are included within the plot. These theoretical results are based upon a classical Bernoulli beam formulation.

In Fig. 7, it is observable that the maximum deflection was registered during the zone B, at which the plate acts as a cantilever. The maximum measured vertical displacement is 40.5 mm. At this point, the theoretical value calculated for a cantilever beam using the elasticity theory is 38 mm. The difference is attributable to the boundary conditions idealized in theory (fully restrained length of the beam while placed on the roller system) as well as to the simplification of the flat launching nose. The experimental test showed that at maximum cantilever stages, the steel plate is not fully supported by the rollers since some gaps were observed (Fig. 8). Consequently,

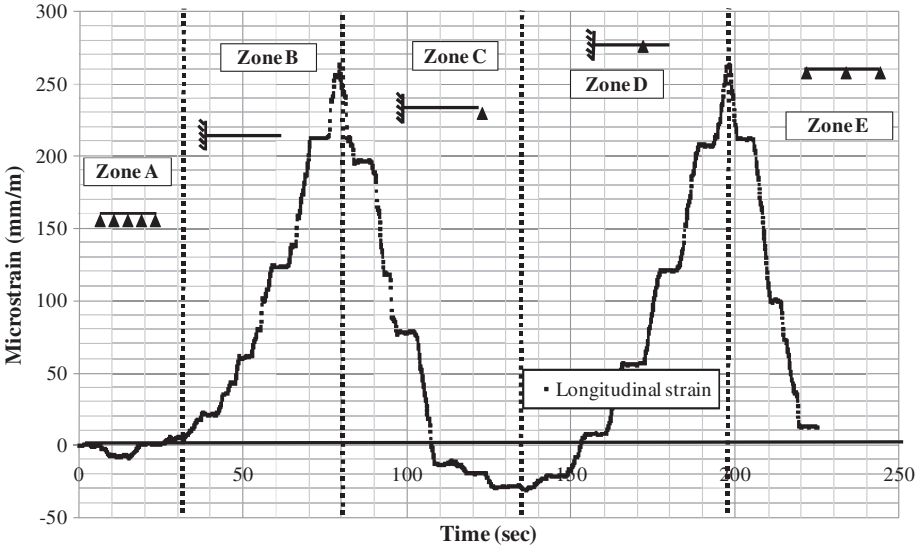

Figure 5 Strain evolution at the upper fiber of the steel plate during the launching.

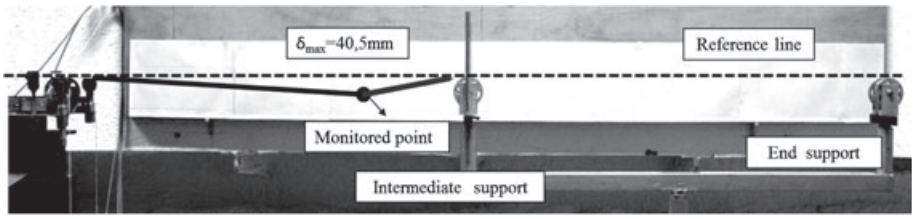

Figure 6 Vertical displacement at monitored point.

the experimentally measured deflection was greater than the one anticipated by the theoretical analysis. Further details concerning the description of the experimental results are given in Ref. 29.

Statistical consistency

A total number of 30 tests were performed. Using the nonparametric Kolmogorov-Smirnov test[30] (K-S) for the maximum strain values obtained at the tracked point in Fig. 6, the sample fitted adequately with a normal distribution. Therefore, the following statistics: mean, standard deviation and variation coefficient were used to describe the experimental sample (Fig. 9). It is observable that the obtained values of maximum strain were reasonably centered on 267 μm/m.

Numerical Reproduction of the Scaled-Reduced ILM

Numerical model

A numerical model implemented in the multi-purpose commercial Software Abaqus-Simulia[31] was used as a numerical simulation tool. The numerical model is based upon the finite element method (FEM) and is able to reproduce a vast spectrum of physical phenomena. In this particular case, the numerical model was expected to reproduce a multi-body physical problem that involved a mechanical interaction between the steel plate and the support conditions (the rollers). Two features characterize the modeling of the phenomenon: the geometrical nonlinearity of the problem and the contact-based formulation of the system.

Several approaches for modeling such mechanical problem were performed throughout the development of the research work.[29] Namely, the approaches included 3D bricks, shells and also beam elements. These approaches differed in various degrees of computational cost, accuracy, collected data, and ease of modeling. Finally, the chosen numerical model was the simplest and less expensive computationally. The chosen model provided a reasonably high level of accuracy when balanced with the amount of collected data, the computational cost, and the usefulness of the results obtained for control and monitoring purposes of incrementally launched steel bridges. Other models (including shells) are under further development and may eventually be useful for monitoring instability-related problems during launching.

The steel plate was modeled with first-order beam elements. The rollers and supports were modeled as

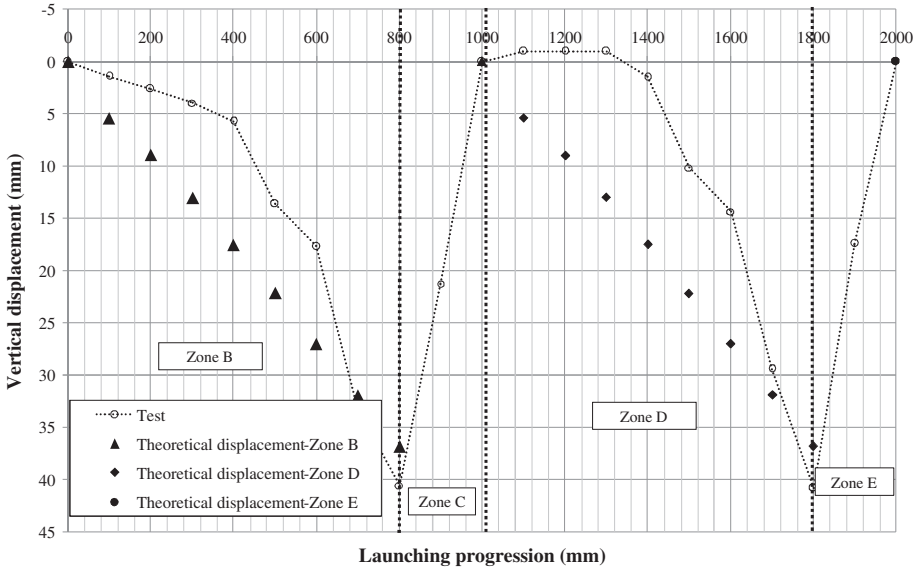

Figure 7 Elastic curve at monitored point.

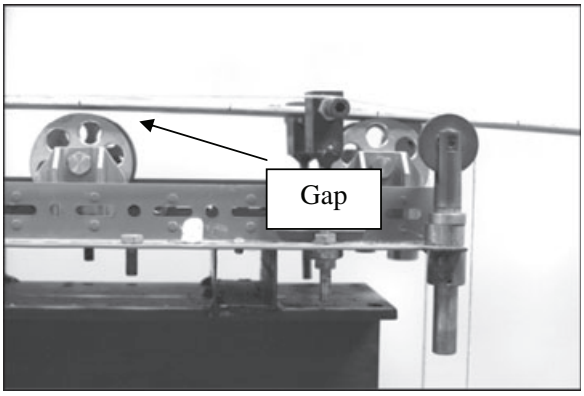

Figure 8 Observable gaps on top of the rollers.

analytical, rigid and frictionless surfaces on which the steel plate was able to slide and/or transmit contact stresses but conversely, was not able to penetrate through. These analytical surfaces were geometrically defined as semicircular objects rigidly connected to the ground. Mathematically, this contact problem is commonly referred to as the penalty-based method. Further mathematical background behind this procedure is available in[29] and in the Software manuals.[31] A convergence analysis by comparing theoretical and experimental values to the numerically obtained ones was also performed. The beam model proved relatively low mesh-dependent. Table 3 shows the principal characteristics of the model, which is simple and straightforward.

Figure 10 displays a lateral view of the numerical reproduction of the scale-reduced test. The point 1 is located precisely at the same position than the strain gages bonded in the steel plate. Consequently, the strain measurements could be compared. The point 2 is located at the beginning of the launching nose and the displacement results (vertical) were compared to those measured at the lab. The numerical model includes thus, a steel plate, 11 rollers as well as the central and end bearings (of the same numerical nature than the rollers).

Validation of the numerical model

The numerical model was validated by reproducing precisely the experimental test depicted in section 3. The experimentally collected data related to strain and vertical displacements was used as a benchmark. The numerical model including the characteristics depicted in Table 3 provided similar results related to strain and vertical displacement as the steel plate was numerically launched. Figure 11 displays the comparison between the experimental and the numerical results related to the longitudinal strain of the steel plate at the depicted point 1. Both curves practically coincide (stepwise nature of the experimental results aside). The numerical model reproduces quite satisfactorily the response observed experimentally both qualitatively and quantitatively. A slight difference between the maximum strain values at both monitored peaks is observable. This difference is attributed to the greater flexibility of the experimental test (Fig. 8)

Figure 12 displays a comparison between the experimental and the numerical results related to the vertical displacement of the steel plate at the depicted point 2. Both curves practically coincide qualitatively

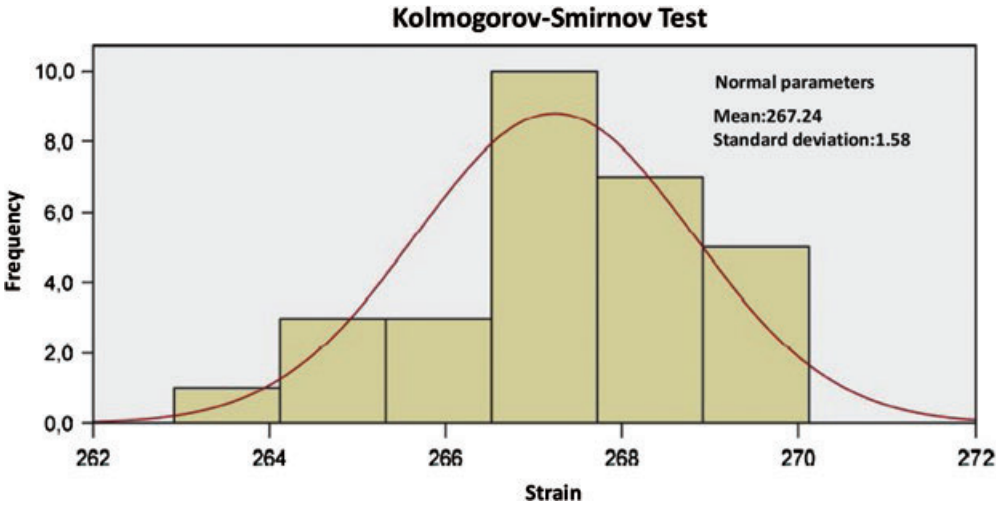

Figure 9 Frequency of the obtained values (maximum recorded microstrain).

Table 3 Characteristics of the numerical model,[29,31]

Numerical simulation	
Software	Abaqus
Solver	Abaqus-Standard
Cross-section	60 mm × 4 mm
Material	Steel
E (N/mm^2)	210,000
Density (kg/m^3)	7850
Constitutive equation (Elastic)	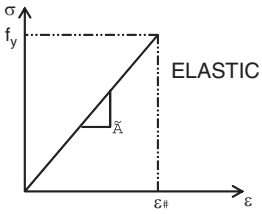
Procedure	Geometrically nonlinear
Contact-friction interaction	Penalty-based contact
	Tangentially: Frictionless
	Normally: No penetration but separation
Load type	Self-weight
Beam element	B21 first-order, planar
$L_{\text{span,scale-reduced}}$ (mm)	2000
Mesh	Uniform, Length= L_{beam}/200
Bearings	Semicircular rigid wires

but there is a difference in quantitative terms when compared to the strain results at peak points. The differences are, however, rather small. The numerical model yields a slightly more flexible response than the experimental data.

The main novel feature of the numerical model, which is the contact-based formulation between the rollers and the girders, is adequately reproduced.

Numerical Reproduction of a Real-Scale Incrementally Launched Bridge

A numerical reproduction of a hypothetical ILM of the steel bridge depicted in Fig. 2 was performed with the validated model. The numerical characteristics of such model are identical to those depicted in Table 3. There is, though, a difference worth mentioning: the bearings in this model were created according to the standard dimensions for these devices.[23] These elements were equally modeled as analytical, rigid surfaces. In this case, a regular mesh of 186 first-order beam elements (B21, whose length equals approximately the relationship $L_{\text{span}}/200$) was deployed. The configuration of the launched structure is identical to the one depicted in Fig. 10 but in this case, $L = 75{,}000$ mm.

The numerical model allows the user to extract any kind of information related to the stress, strain, displacement, and the contact forces fields. This represents a vast amount of data, which is not necessarily useful during the construction stages. In field bridge engineering, it might be of great usefulness to accurately anticipate the forces, strains, and displacements the girder undergoes during the incremental launching procedure. Consequently, the results that are displayed herein are aimed at showing the potential control tools such simulation may provide. Therefore, three structural results are monitored and depicted:

- Strains at point A (exact middle point of the girder).
- Vertical displacement at the front of the cantilever.
- Reaction forces at central and end bearings.

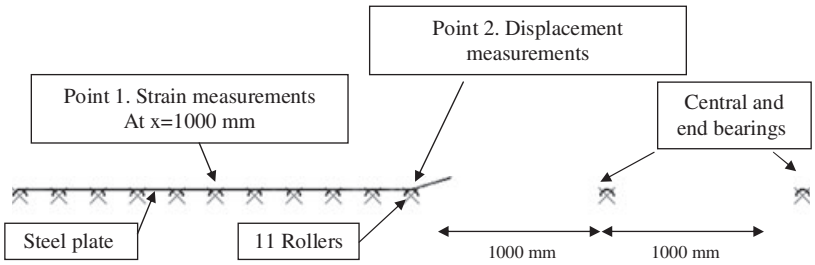

Figure 10 Numerical reproduction of the scale-reduced test. Lateral view.

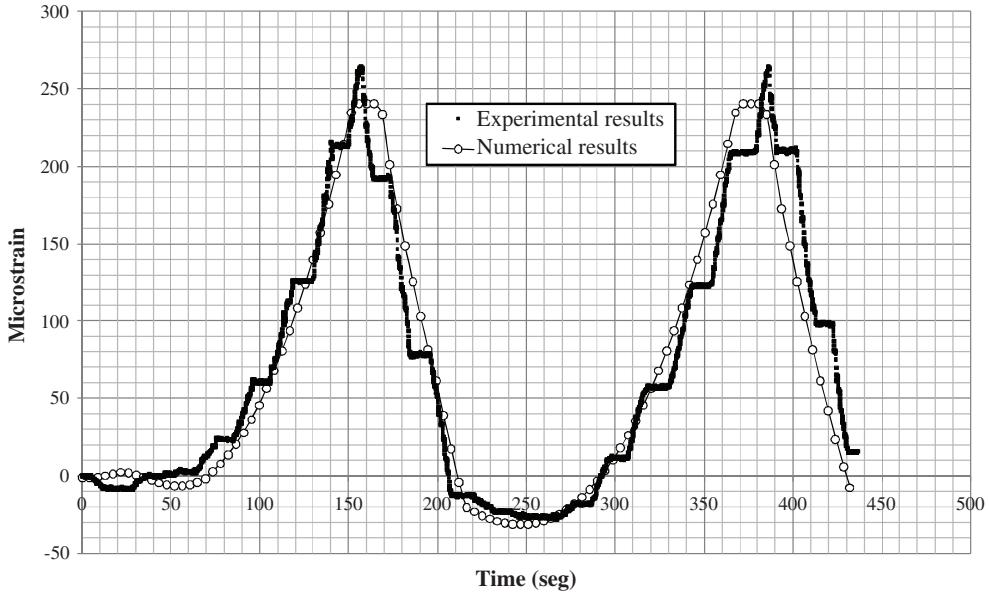

Figure 11 Numerical versus experimental results related to longitudinal strain.

The above-mentioned magnitudes are usually monitored during the launching phase. A thorough comparison between the anticipated values and the field measurements may clarify and/or confirm the correct practice of the launching process or potentially, may prevent undesired problems during construction.

Strains

The results concerning stresses and strains are useful in a twofold fashion:

- For design purposes, the model may warn about any potential yielding of the girder during the ILM if the strain is associated with the constitutive equation of the material.
- For control purposes, the results related to strains may be compared with in situ measurements that are increasingly used nowadays.[20–23]

For the former, localized yielding of the steel girders during launching is highly undesired. The numerical model provides information that may anticipate any potential yielding of the girder at any point. The numerical model may flag any finite element that overpasses a defined threshold of stresses (namely, the yield stress f_y). The yielded areas could be pinpointed at the end of the procedure and the design of the steel girder may be changed at design stages.

For the latter, the model allows to track the strain at any given point of interest (that may be the points at which strain gages are located). The stress levels may also be inferred from the strain field via the constitutive equation (which is reasonably expected to be linear during construction).

Figure 13 displays a control plot of strain and stresses obtained with the numerical simulation of the ILM. The strain–stress values are obtained from point A, which is located where the maximum longitudinal stress occurs.

Noticeably, sign reversals are observable since the girder undergoes consecutive sagging and hogging bending moments. This information should reasonably coincide with the field measurements. Finally,

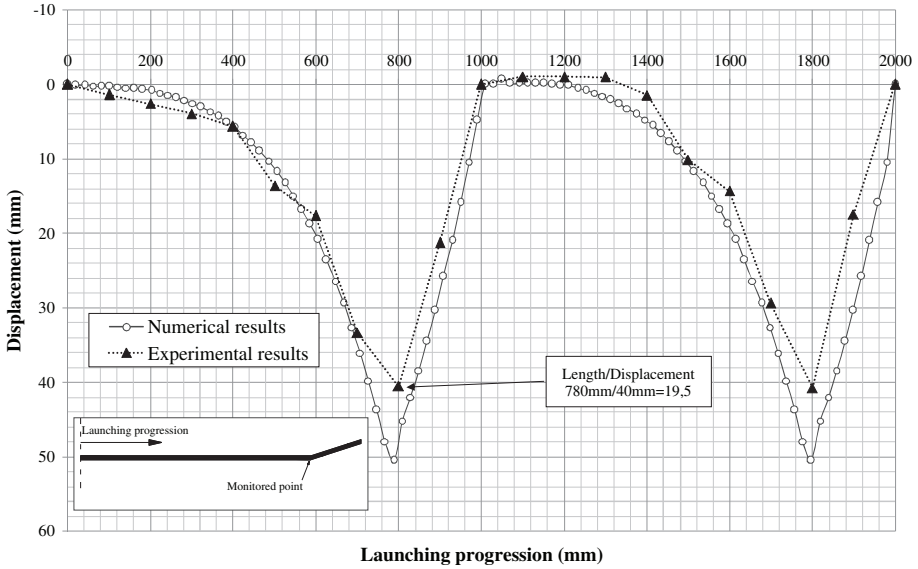

Figure 12 Numerical versus experimental-vertical displacement.

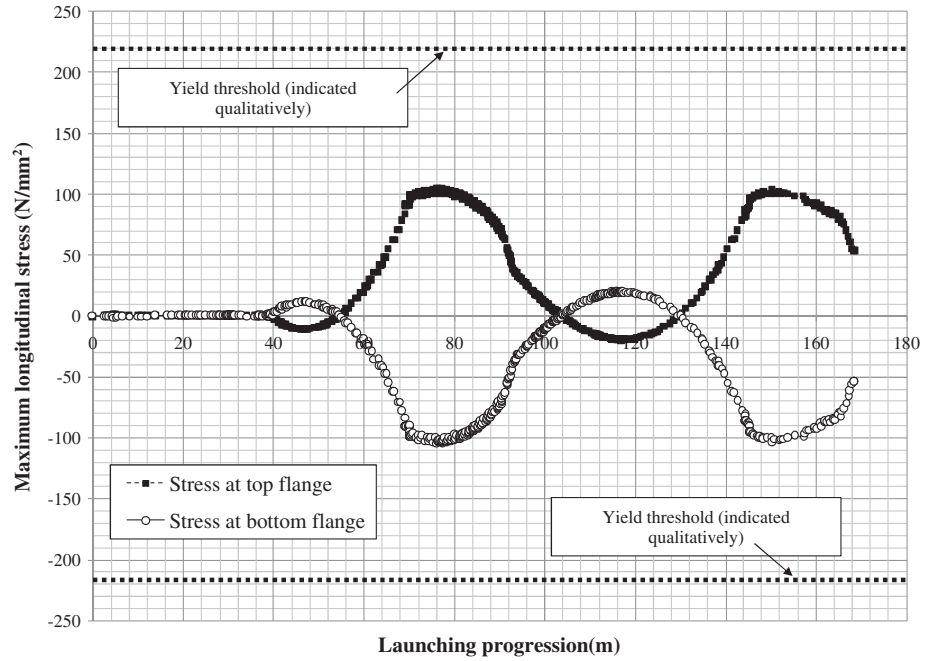

Figure 13 Longitudinal stress control at point A.

the plot includes thresholds that define warning areas of undesired levels of stress and strain (pinpointed qualitatively in the plot).

Vertical displacements

The vertical displacements of the steel girders are generally monitored and controlled in situ with basic topographic equipment. These measurements do not require complex acquisition data systems despite the high level of accuracy provided by modern total stations. The contractors, designers and bridge owners often rely on such measurements due to their adequate balance between accuracy and ease. Any individual involved in the construction can track the progression of the launching in terms of deflection of the steel girder.

Figure 14 displays the history of the vertical displacement of the point referred to as B in the plot obtained with the numerical model. This history should be read as follows, for a given distance x (mm) of the tracked point during launching, its vertical displacement is given. Noticeably, the displacement increases in sagging zones and decreases as the girder

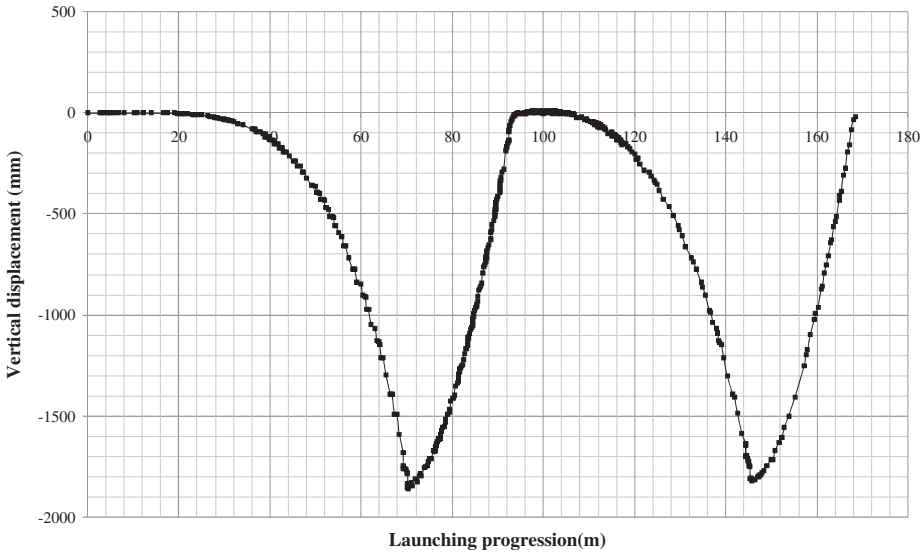

Figure 14 Vertical displacement control of a real-scale launched steel bridge.

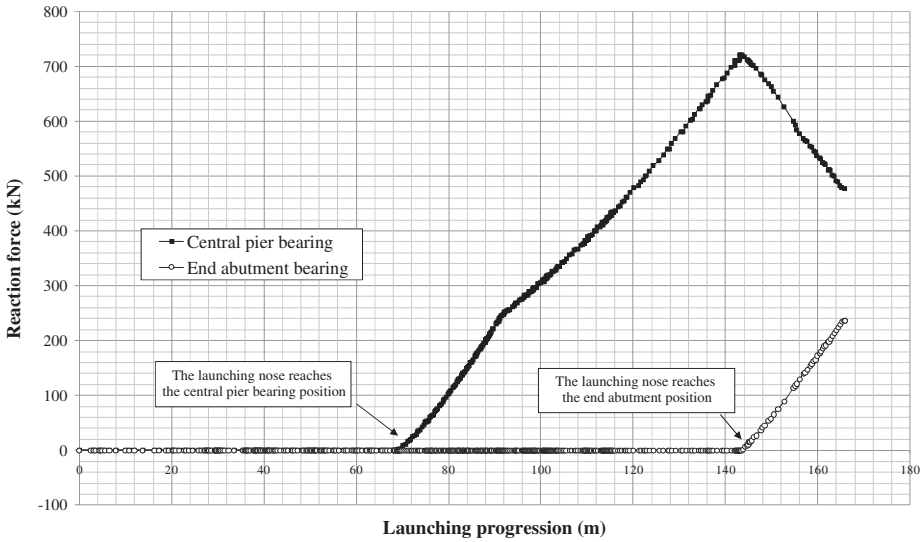

Figure 15 Vertical reaction control at central pier and end abutment.

passes over a given bearing. Field measurements and numerical predictions may also be compared and thus, conclusions related to the process may be drawn.

Reaction force at the bearings

Load cells are usually deployed at bearing during launching.[32] These measurements allow to monitor the magnitude of the reaction forces. In bridges with multigirder cross-sections, these measurements are of the utmost importance for the verification of the adequate position of the bridge during launching. All load cells provided at a given bearing should read a proportional amount of the total load which is known beforehand. If an undesired loss of symmetry occurs during launching, the reactions forces would differ considerably from one girder to another. This implies repositioning of the bridge with all costs and time-waste associated.

The numerical model provides information related to the contact stresses transmitted from the girders to the bearing. In addition, it provides information related to the internal forces that occur at the girder (bending moment, shear). Figure 15 displays a reaction force graph plotted against the distance at which the launching nose is located (namely, the launching progression). The results might be compared with in situ measurements for control purposes but also, these results might be used at design stages. In steel launched bridges, it is well-known that the patch loading forces combined with the bending moments are, among others, important forces to be verified.

Conclusions

In this paper, experimental and numerical models aimed at stimulating the structural behavior of a steel I-girder bridge constructed by the ILM are depicted.

On one hand, the experimental test has been performed in a scale-reduced fashion and has been useful for validation purposes. On the other hand, the numerical model using beam elements proves versatile when simulating the launching process within a short calculation time. The numerical model includes a contact-based formulation which reproduces satisfactorily the transient support conditions that occur during the ILM.

The numerical simulation of the ILM represents a useful tool for monitoring and controlling the various magnitudes that are typically measured in situ with traditional field equipment. This numerical control allows bridge designers, contractors, and owners to anticipate the structural response of the steel girders. Results related to the strain–stress field, vertical displacements, and reaction forces at bearings might be easily inferred from the simulation and compared to field measurements. The proposed simulation of the ILM model provides an adequate balance between accuracy, collected data, and ease. The simulation presented herein might be extended to box girders or other bespoken cross-sections.

References

1. LaViolette, M., Wipf, T., and Lee, Y., *Bridge Construction Practices Using Incremental Launching, American Association of State Highway and Transportation Officials, AASHTO*, Ames, Iowa (2007).
2. Rosignoli, M., *Bridge Launching, Thomas Telford*, London, UK (2002).
3. Baur, W., ''Bridge Erection by Launching is Fast, Safe and Efficient,'' *Civil Engineering–ASCE* **47**(3): 60–63 (1977).
4. Gohler, B., and Pearson, P., *Incrementally Launched Bridges. Design and Construction, Ernst and Sohn*, Berlin (2000).
5. Alistair, P., *Large and Small Incrementally Launched Structures, Transportation Research Record 1696 (5B0060), Transportation Research Board*, Washington D.C. (2000).
6. Zellner, W., and Svensson, H., ''Incremental Launching of Structures,'' *Journal of Structural Engineering* **109**(2): 520–537 (1983).
7. Rosignoli, M., ''Site Restrictions Challenge Bridge Design,'' *Concrete International* **20**(8): 40–44 (1998).
8. Rosignoli, M., ''Pre-sizing of Prestressed Concrete Launched Bridges,'' *ACI Structural Journal* **96**(5): 705–711 (1999).
9. Rosignoli, M., ''Nose-Deck Interaction in Launched Prestressed Concrete Bridges,'' *Journal of Bridge Engineering* **3**(1): 21–27 (1998).
10. Rosignoli, M., ''Reduced-Transfer-Matrix Method of Analysis of Launched Bridges,'' *ACI Structural Journal* **96**(4): 603–608 (1999).
11. Rosignoli, M., ''Monolithic Launch of the Reggiolo Overpass,'' *Concrete International* **29**(2): 26–30 (2001).
12. Granath, P., ''Distribution of Support Reaction Against a Steel Girder on a Launching Shoe,'' *Journal of Constructional Steel Research* **47**(3): 245–270 (1998).
13. Granath, P., Thorsson, A., and Edlund, B., ''I-Shaped Steel Girders Subjected to Bending Moment and Travelling Patch Loading,'' *Journal of Constructional Steel Research* **54**(3): 409–421 (2000).
14. Granath, P., ''Serviceability Limit State of I-Shaped Steel Girders Subjected to Patch Loading,'' *Journal of Constructional Steel Research* **54**(3): 387–408 (2000).
15. Favre, R., Badoux, M., Burdet, O., and Laurencet, P., ''Incremental Launching for the Ile Falcon Bridge,'' *Concrete International* **21**(2): 46–51 (1999).
16. Hewson, N., and Hodgkinson, A., ''Incremental Launch of Brides Glen Bridge, Ireland, Concrete,'' *Vol.* **38**(7): 29–31 (2004).
17. Zhuravov, L., Chemerinsky, O., and Seliverstov, V., ''Launching Steel Bridges in Russia,'' *Journal of International Association for Bridge and Structural Engineering (IABSE)* **6**(3): 183–186 (1996).
18. Marzouk, M., El-Dein, H., and El-Said, M., ''Application of Computer Simulation to Construction of Incrementally Launching Bridges,'' *Journal of Civil Engineering and Management* **13**(1): 27–36 (2007).
19. Xu, R., and Shao, B., ''A New Beam Element for Incremental Launching of Bridges,'' *Journal of Bridge Engineering* **17**(5): 1–19 (2011).
20. Chacón, R., Guzmán, F., Mirambell, E., Real, E., and Oñate, E., ''Wireless Sensor Networks for Strain Monitoring During Steel Bridges Launching,'' *International Journal of Structural Health Monitoring* **8**(3): 195–205 (2009).
21. Wipf, T., Phares, B., Abendroth, R., Chang, B., Abraham, S., ''Monitoring of the Launched Girder Bridge over the Iowa River on US 20,'' Final Report CTRE Project 01–108. Center for Transportation Research and Education, Iowa State University, Ames, Iowa (March 2004).
22. Lebet, J., *Measurements Taken During the Launch of the 130 m Span Vaux Viaduct, Steelbridge, OTUA*, Millau (2004).
23. Zhang, Y., and Luo, R., ''Patch Loading and Improved Measures of Incremental Launching of Steel Box Girder,'' *Journal of Constructional Steel Research* **68**(1): 11–19 (2012).

24. Martins, O.P., and Sampaio, A.Z., ''Bridge Launching Construction Visualized in a Virtual Environment,'' *The International Journal of Virtual Reality* **10**(2): 49–56 (2011).
25. Kuhlmann, U. et al. *Combri Design Manual –Part I Applications of Euro Code Rules*, 1st edition, Stuttgart, Germany (2008).
26. Buckingham, E., ''On Physically Similar Systems. Illustrations of the Use of Dimensional Equations,'' *Physical Review* **4**: 345–376 (1914).
27. Blanco, E., Oller, S., and Gill, L., *Análisis Experimental de estructuras*, *CIMNE*, Barcelona (2007 (in Spanish)).
28. *CATMAN Easy V 6.10*, *Hottinger Baldwin Messtechnik HBM*, Darmstadt, Germany (2012).
29. Uribe N. *Reproducción numérica y experimental del proceso de lanzamiento de un puente metálico por empujes sucesivos*, Master's Thesis, Construction Engineering Department, ETSICCPB, Universitat Politècnica de Catalunya (2012) (in Spanish), URL http://upcommons.upc.edu/pfc/handle/2099.1/14898 [accessed on 25 November 2013].
30. Lindgren, B.W., *Statistical Theory*, 2nd Edition, *The Mcmillan Company*, New York (1962).
31. *Abaqus FEA, Simulia© V6.10.3*, Dassault Systèmes, Paris, Boston, Tokyo (2012).
32. Marzouk, M., Said, H., and El-Said, M., ''Framework for Multiobjective Optimization of Launching Girder Bridges,'' *Journal of Construction Engineering and Management* **135**(8): 791–800 (2011).